Nucleic Acids Research, 2005, Vol. 33, No. 8 ***2751–2763***
doi:10.1093/nar/gki576

RNR1, a 3′–5′ exoribonuclease belonging to the RNR superfamily, catalyzes 3′ maturation of chloroplast ribosomal RNAs in *Arabidopsis thaliana*

Thomas J. Bollenbach, Heike Lange[1], Ryan Gutierrez, Mathieu Erhardt[1], David B. Stern* and Dominique Gagliardi[1]

Boyce Thompson Institute for Plant Research, Cornell University, Tower Rd., Ithaca, NY 14853, USA and [1]Institut de Biologie Moléculaire des Plantes, CNRS UPR2357, 12 rue du général Zimmer, 67084 Strasbourg cedex, France

Received March 23, 2005; Revised and Accepted April 26, 2005

ABSTRACT

Arabidopsis thaliana **chloroplasts contain at least two 3′ to 5′ exoribonucleases, polynucleotide phosphorylase (PNPase) and an RNase R homolog (RNR1). PNPase has been implicated in both mRNA and 23S rRNA 3′ processing. However, the observed maturation defects do not affect chloroplast translation, suggesting that the overall role of PNPase in maturation of chloroplast rRNA is not essential. Here, we show that this role can be largely ascribed to RNR1, for which homozygous mutants germinate only on sucrose-containing media, and have white cotyledons and pale green rosette leaves. Accumulation of chloroplast-encoded mRNAs and tRNAs is unaffected in such mutants, suggesting that RNR1 activity is either unnecessary or redundant for their processing and turnover. However, accumulation of several chloroplast rRNA species is severely affected. High-resolution RNA gel blot analysis, and mapping of 5′ and 3′ ends, revealed that RNR1 is involved in the maturation of 23S, 16S and 5S rRNAs. The 3′ extensions of the accumulating 5S rRNA precursors can be efficiently removed *in vitro* by purified RNR1, consistent with this view. Our data suggest that decreased accumulation of mature chloroplast ribosomal RNAs leads to a reduction in the number of translating ribosomes, ultimately compromising chloroplast protein abundance and thus plant growth and development.**

INTRODUCTION

Development of chloroplasts from proplastids and expression of the plastid genome are intimately linked processes, which are ultimately coordinated by nucleus-encoded proteins and enzymes. Chloroplast gene expression is regulated at several steps, one of these being post-transcriptional RNA processing. This includes endonucleolytic cleavage of long polycistronic transcripts, and 5′ and 3′ end processing of precursor RNAs (1).

A heavily processed transcript in the plastids of flowering plants is the polycistronic primary transcript emanating from the ribosomal RNA (rrn) operon. This highly conserved gene cluster encodes the 16S, 23S, 4.5S and 5S rRNAs and three tRNAs. Maturation of the primary transcript occurs via a series of endo- and exonucleolytic steps. The primary precursor is initially processed by excision of the tRNAs and by additional endonucleolytic cleavages to generate 16S and 5S rRNA precursors, and a dicistronic 23S–4.5S processing intermediate. Subsequent endonucleolytic processing of the 23S–4.5S rRNA to generate monocistronic 23S and 4.5S rRNAs appears to occur on the ribosome [(2), reviewed in (3)] and is thought to require prior 3′ end maturation of 4.5S rRNA (4). The 16S, 23S and 5S rRNA precursors generated by endonucleolytic cleavage require further processing to establish mature 5′ and 3′ ends.

While the molecular nature of rRNA processing has been gradually elucidated, the nature of the enzymatic machinery has remained elusive, in part because certain rRNA defects can represent pleiotropic effects where plastid biogenesis has been otherwise impaired (5). Several higher plant mutations, however, appear to have a primary defect in the processing of plastid rRNAs. For example, the maize mutant *hcf7* is impaired in 16S rRNA 5′ and 3′ end processing, and the *Arabidopsis* mutant *dal1* is impaired in the processing of 16S rRNA 3′ ends and accumulates the 23S–4.5S dicistronic processing intermediate (5,6). The *Arabidopsis* mutant *wco* is also affected at least in 16S rRNA processing, but this defect is observed only in cotyledons (7). The *DCL* gene is essential for the accumulation of mature chloroplast ribosomes in

*To whom correspondence should be addressed. Tel: +1 607 254 1306; Fax: +1 607 254 6779; Email: ds28@cornell.edu

Arabidopsis and tomato (2,8); however, defects in ribosomal proteins do not necessarily lead to aberrant rRNA processing (9,10). None of the genes affected by the mutations discussed above encodes proteins resembling known RNA processing factors, although DCL does interact with known RNA processing enzymes (8). An apparent exception to these findings is the phosphorolytic 3′ to 5′ exoribonuclease, polynucleotide phosphorylase (PNPase), whose chloroplast isozyme (At3g03710) has been implicated in 23S rRNA 3′ end processing (11). This leaves open the question of how chloroplast rRNA maturation is regulated, and whether this maturation is linked to other processes.

The RNR superfamily of hydrolytic 3′ to 5′ exoribonucleases, which includes the prokaryotic enzymes RNase II, is, in prokaryotes, primarily involved in the turnover of mRNA and of polyadenylated RNA degradation intermediates (12). RNase R, together with PNPase, is involved in the turnover of 16S and 23S rRNA degradation intermediates (13), and highly structured RNAs (12). The *Arabidopsis* nuclear genome encodes three members of the RNR superfamily, which we have named RNR1-3. *Arabidopsis* RNR1 (At5g02250), previously named AtmtRNaseII, was first implicated in the final step of mitochondrial *atp9* mRNA 3′ end maturation (14). This enzyme was subsequently shown to also be chloroplast-targeted in *Arabidopsis*, and it was observed that a weak mutant allele of *RNR1* led to the accumulation of the 23S–4.5S processing intermediate (15). Here, we demonstrate, using null mutants, that RNR1 plays a profound role in rRNA metabolism, and thus in plant development.

MATERIALS AND METHODS

Plant material and growth conditions

The WT ecotype Columbia (Col-0) of *Arabidopsis thaliana* was used in this study. Three *rnr1* mutant lines, SALK_138535 (*rnr1-1*), SALK_044726 (*rnr1-2*) and SALK_090294 (*rnr1-3*), containing T-DNA insertions in the gene At5g02250, were obtained from the SIGnAL mutant collection (16). Mutant plants and WT controls were germinated and grown on MS agar (17) supplemented with 0.5% (w/v) sucrose, under fluorescent lights (50 $\mu mol \cdot m^{-2}\ s^{-1}$) and a 16 h-light/8 h-dark photoperiod. The precise locations of the T-DNA left borders were determined by sequencing of DNA amplified by PCR from plants carrying the mutant alleles.

Electron transmission microscopy analysis

Cotyledon tissue samples were fixed overnight in 3% glutaraldehyde and then treated for 2 h with 10% (w/v) picric acid, 2 h with 2% uranyl acetate and stained with 0.1% (v/v) osmium tetroxide in 150 mM phosphate buffer, pH 7.2. Samples were then dehydrated through an ethanol series and infiltrated with EPON812 medium grade resin (Polysciences, Germany). Polymerization was allowed to proceed for 48 h at 60°C, after which ultrathin sections (90 μm) were cut using an Ultracut E microtome (Reichert) and collected on grids coated with formvar (EMS, WA). Samples were visualized with a Hitachi H-600 electron microscope operating at 75 kV.

RNA isolation and RT–PCR analysis of RNR1 expression in WT and rnr1 plants

RNA was extracted with Trizol (Sigma, St Louis, MO) according to the manufacturer's instructions. For RT–PCR, *RNR1* cDNA was generated from 1 μg total RNA from WT plants using AMV RT and the primer RNR3′ (Table 1) according to the manufacturer's instructions (Promega, Madison, WI). Aliquots were added to a PCR containing the primers RNR3′ and RNR5′ and amplified with Takara ExTaq according to the manufacturer's instructions (Takara Shuzo, Kyoto, Japan). PCR was performed for 28 cycles with the following program: denaturation at 95°C for 30 s, annealing at 55°C for 30 s and extension at 72°C for 1 min. The ubiquitin *UBQ10* transcript was amplified in the same reaction as an internal control, using the primers UBQ1 and UBQ2.

RNA gel blot analysis

To measure chloroplast transcript accumulation, 1 μg of total RNA from WT and *rnr1* plants was separated in 1.2% agarose/3% formaldehyde gels and blotted onto HyBond N^+ (Amersham Biosciences, Piscataway, NJ) by capillary transfer in 25 mM phosphate buffer. Following UV-crosslinking in a Stratalinker (Stratagene, La Jolla, CA), membranes were prehybridized in Church and Gilbert buffer (18) for at least 30 min before incubation overnight with radiolabeled gene-specific probes. For high-resolution analysis, 1.5 μg total RNA from WT and *rnr1* plants was analyzed using 12% (w/v) acrylamide–bisacrylamide (19:1)/7 M urea gels as described previously (19). The probes are described in the Figures 3, 4, 7, 8 and 11 and associated legends. For polysome analysis, sedimentation of crude cell lysates through 15–55% sucrose gradients was performed as described previously (5,20). RNA gel blot analysis of gradient fractions was performed as described above.

Table 1. Sequences of oligonucleotide primers used in this study[a]

Primer	Sequence (5′ to 3′)
16-R1 cDNA	GTATTAGCAGCCGTTTCCAG
16-R2 PCR	TCCCAAGGGCAGGTTCTTAC
16-F1 PCR	TAATCGCCGGTCAGCCATAC
23-R1 cDNA	GGATTCAGCAGCAGTTCAAAAG
23-R2 PCR	GCATTTCGTCGCTTACTACG
4.5-F1 PCR	AGCTGAGGCATCCTAACAGAC
5SR1 cDNA	ACCGCAGTAGAGTTTAACCACC
5SR2 PCR	CAAGTTCGGGATGGATTG
5SF1 PCR	ACGATACTGTAGGGGAGGTC
T75S	**T7**-TATTCTGGTGTCCTAGGCGTAG
5S Reverse	ATCCTGGCGTCGAGCTATT
5S + 20 Reverse	AGGTGTTAAGCTTTTCATC
RNR3′	AAGAAGAGCTTCAGCAGCTTCAGTG
RNR5′	TCGATCAATATATAGCCCTCGGCCT
UBQ1	GATCTTTGCCGGAAAACAATTGGAGGATGGT
UBQ2	CGACTTGTCATTAGAAAGAAAGAGATAACAGG
23S-5′	CGGTAAACGCTGGGTAGCCAAGTGCGGAGCGG
23S-3′	**T3**-CCTCTTGAATTCTCAAAACTTC
4.5S-5′	AAGGTCACGGCGAGACGAGCCGTT
4.5S-3′	**T3**-ATCGAACCATGAACGAAGAAAG
5S-5′	ATTCTGGTGTCCTAGGCGTAGAGG
5S-3′	**T3**-CACCCCGTCTCCACTGGA

[a]Positions of T3 and T7 promoter sequences are indicated in bold.

RNase protection

Templates for the RNA probes used in this analysis were PCR-amplified from *Arabidopsis* total DNA. A 207 nt 23S template was amplified using the primers 23S-5′ and 23S-3′, a 374 nt 4.5S template was amplified using the primers 4.5S-5′ and 4.5S-3′, and a 376 nt 5S template was amplified using the primers 5S-5′ and 5S-3′. The resulting PCR products, which encode a T3 RNA polymerase promoter, were used to synthesize probes *in vitro* as described previously (21). S1 hybridization buffer (40 mM PIPES, pH 6.4, 1 mM EDTA, 400 mM NaCl and 85% formamide), total RNA from WT or *rnr1* plants, or yeast tRNA and either 23S, 4.5S or 5S RNA probes were mixed, and the assay was carried out as described by Monde *et al*. (22) with the exception that overnight hybridization was carried out at 42°C, and digestion of single-stranded RNA was carried out at 4°C for 30 min. Reaction products were resolved in 6% denaturing polyacrylamide gels and were visualized and quantified using a Storm scanner (Molecular Dynamics, Sunnyvale, CA).

Circular RT–PCR

The precise 5′ and 3′ ends of the 16S rRNA, 5S rRNA and 23S–4.5S rRNA precursors were determined using circular RT–PCR (cRT–PCR) as described previously (19). Briefly, total RNA was circularized using T4 RNA ligase (New England Biolabs), and cDNA spanning the junction of the 5′ and 3′ ligated ends was synthesized using gene-specific reverse primers (Table 1). This region was then amplified by PCR using gene-specific primers, cloned into pCR2.1 TOPO (Invitrogen) and sequenced.

In vitro assay of purified RNR1

The purification and assay of RNR1 were performed as described previously (14). Templates for *in vitro* transcription were generated by amplifying the 5S gene from *Arabidopsis* DNA using the primers T7 5S and 5S Reverse, to generate the mature 5S rRNA substrate, or T7 5S and 5S + 20 Reverse, to generate the pre-5S rRNA substrate containing a 20 nt extension.

Protein isolation and immunoblotting

Tissue from 40-day-old plants was ground to a fine powder in liquid nitrogen and allowed to thaw in extraction buffer (10 mM Tris–HCl, 18% sucrose, 10 mM $MgCl_2$, 1% 2-mercaptoethanol and 1% SDS). Debris was pelleted by centrifugation and an equal volume of 2× SDS–PAGE loading buffer was added to the supernatant. Loading of proteins was calibrated by measuring total absorption at 280 nm.

RESULTS

RNR1 T-DNA insertion mutant analysis

The *Arabidopsis* nuclear gene At5g02250 encodes a 782 amino acid protein possessing an RNB domain (Pfam domain PF00773), which is found in at least 274 proteins related to RNase II and RNase R (23). The exoribonucleolytic activity of the At5g02250 gene product was confirmed following the purification of a C-terminal tagged version from overexpressing transgenic *Arabidopsis* plants (14,19). The At5g02250 product was first named AtmtRNase II based on its mitochondrial localization as determined by transient expression of a fusion of the N-terminal 192 amino acids to green fluorescent protein (GFP), and the observation that an increased number of incompletely processed mitochondrial *atp9* mRNA 3′ ends accumulated in mutant plant, based on sequencing of cRT–PCR products (14).

However, a chloroplast localization was subsequently proposed for this same protein, when a GFP fusion to 118 N-terminal amino acids was expressed, also in *Arabidopsis* (15). These workers further showed that a T-DNA insertion 36 bp upstream of the At5g02250 translation initiation codon gene decreased, but did not abolish expression, and resulted in plants exhibiting impaired photosynthesis, retarded growth and pale green leaves. Given that the GFP results and growth phentoypes suggested a role for At5g02250 in chloroplast biogenesis, the gene was re-named *RNR1*, a nomenclature that we have adopted here. However, the participation of *RNR1* in cpRNA metabolism was not thoroughly explored.

To pursue the analysis of *RNR1* in the context of chloroplast biogenesis, we selected three T-DNA insertion alleles from the Salk SIGnAL collection, naming them *rnr1-1* (SALK_138535), *rnr1-2* (SALK_044726) and *rnr1-3* (SALK_090294) (Figure 1A). Homozygous mutants from

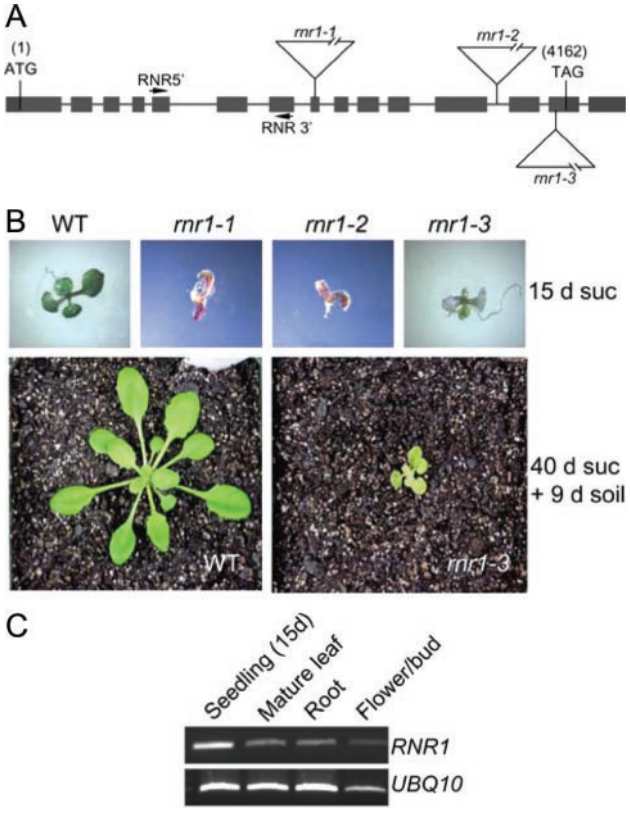

Figure 1. *RNR1* T-DNA insertion mutants. (**A**) Diagram of the *RNR1* gene showing the positions of three T-DNA insertion alleles used in this work. The positions of T-DNA insertions were confirmed by PCR. (**B**) WT and homozygous *rnr1* mutants were germinated on sucrose-containing media for 15 days (top panels), or grown on sucrose-containing media for 40 days and transferred to soil for an additional 9 days (bottom panels). (**C**) RT–PCR showing expression of the *RNR1* gene in different tissues of WT *Arabidopsis*. Primers used in this analysis (RNR5′ and RNR3′) are indicated in (A).

each line were isolated following three outcrosses of the original T3 plants. Homozygous plants from each of these lines required germination and initial growth on sucrose-containing medium, consistent with a defect in photosynthesis. Figure 1B compares WT and *rnr1* homozygotes after 15 days of growth on MS sucrose. The cotyledons of *rnr1* plants emerged either white or dark red, signifying a lack of chlorophyll and a significant accumulation of anthocyanins, which dissipated after several days as the cotyledons became white and then pale green (Figure 1B, top panels). The rosette leaves of *rnr1* mutants, which are already visible in *rnr1-3* seedlings after 15 days, emerged and remained pale green compared with those of WT plants.

Following 40 days of growth on MS sucrose, both WT and *rnr1-3* were transferred to soil and were grown for an additional 9 days (Figure 1B, bottom panels). Under these conditions, growth of *rnr1-3* was significantly slower than the WT, and rosette leaves of the mutant remained pale green. Fourteen-day-old etiolated WT and *rnr1* plants were indistinguishable, which indicated that RNR1 activity was not required for skotomorphogenesis (data not shown), and the roots of the *rnr1* plants resembled those of the WT at all stages of growth.

Given the strong effect of the *rnr1* mutations on green tissues, it was of interest to determine whether *RNR1* exhibited tissue-specific expression. RT–PCR was used to determine the mRNA abundance for *RNR1* in WT seedlings, mature leaves, roots and flower/flower buds (Figure 1C). The highest expression was found in 15-day-old seedlings, and roughly uniform expression was found in the other tissues examined, as compared with the control ubiquitin transcript. This result would be consistent with the presence of RNR1 in mitochondria (14,19), which are active in gene expression in non-green tissues. The extent to which RNR1 is required in plastid types other than chloroplasts is unknown.

To confirm the defect in chloroplast biogenesis suggested by the pale leaves of *rnr1* plants, cotyledons of WT and *rnr1* plants were observed by light and transmission electron microscopy (TEM), as shown in Figure 2. Following toluidine blue staining of transverse sections of cotyledons, chloroplasts could be detected in WT but not in *rnr1* cotyledons (Figure 2A). Furthermore, *rnr1* cotyledons exhibited a severely disorganized structure with no recognizable lower epithelium. Further analysis by TEM revealed that *rnr1* plastids contained no stacked thylakoids, and that these leaves contained plastoglobules (Figure 2B), the latter perhaps reflecting a stress response. Taken together, these data suggest that RNR1 is essential for chloroplast development in cotyledons, and that this requirement is less strict in rosette leaves.

mRNA and tRNA transcripts accumulate normally in rnr1 plants

Because RNase II and RNase R are important for regulating RNA processing and turnover in bacteria, we compared the accumulation of representative mRNAs and tRNAs in 40-day-old WT and *rnr1* plants grown on sucrose-containing medium. We observed no differences in the accumulation of mRNAs encoding the α-subunit of the CF_0CF_1 ATPase complex (*atpA*), the Photosystem II D1 protein (*psbA*), the Rubisco large subunit (*rbcL*), or of a tricistronic mRNA encoding the PsaA/PsaB subunits of Photosystem I and the ribosomal S14 subunit (*psaA-psaB-rps14*) (Figure 3A). We also observed no difference in the accumulation of the mitochondrial mRNA *cox3*, which encodes cytochrome oxidase subunit III. The *rnr1* mutation also had no obvious effect on 3′ end processing of *psbA* or *rbcL* transcripts, a phenotype that has been observed previously in chloroplast PNPase-deficient *Arabidopsis* (11). RNA gel blots were also probed to detect an intronless tRNA, $tRNA^{Phe}$ (*trnF*), and an intron-containing tRNA, $tRNA^{Leu}$ (*trnL*). As shown in Figure 3A, we observed no differences—neither in the accumulation of $tRNA^{Phe}$ nor in the accumulation of the precursor or mature forms of $tRNA^{Leu}$. RNR1 activity is, therefore, redundant or not required for processing and turnover of chloroplast mRNA and tRNA.

rnr1 plants accumulate fewer photosynthetic proteins than WT

The pale leaf phenotype of the *rnr1* mutants (Figure 1B) and microscopic evidence for a defect in chloroplast development (Figure 2) suggested that although chloroplast mRNAs were accumulating normally (Figure 3A), *rnr1* was not

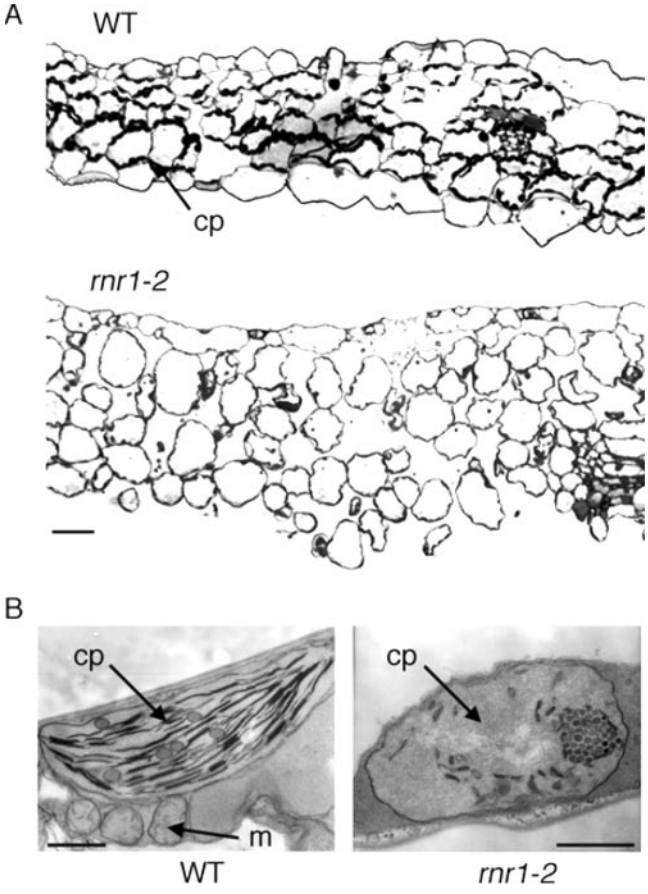

Figure 2. Loss of *RNR1* expression affects chloroplast biogenesis. (**A**) Transverse sections of cotyledons from 3-week-old WT and *rnr1* plants stained with toluidine blue. Chloroplasts (cp) are visible in WT cotyledons as globular shapes. *rnr1* cotyledons exhibit a severely disorganized structure and contain no visible chloroplasts. The magnification bar corresponds to 100 μm. (**B**) Transmission electron micrographs from cotyledons of 3-week-old WT and *rnr1* plants. Mitochondria and plastids are indicated by m and cp, respectively. The magnification bars correspond to 1 μm.

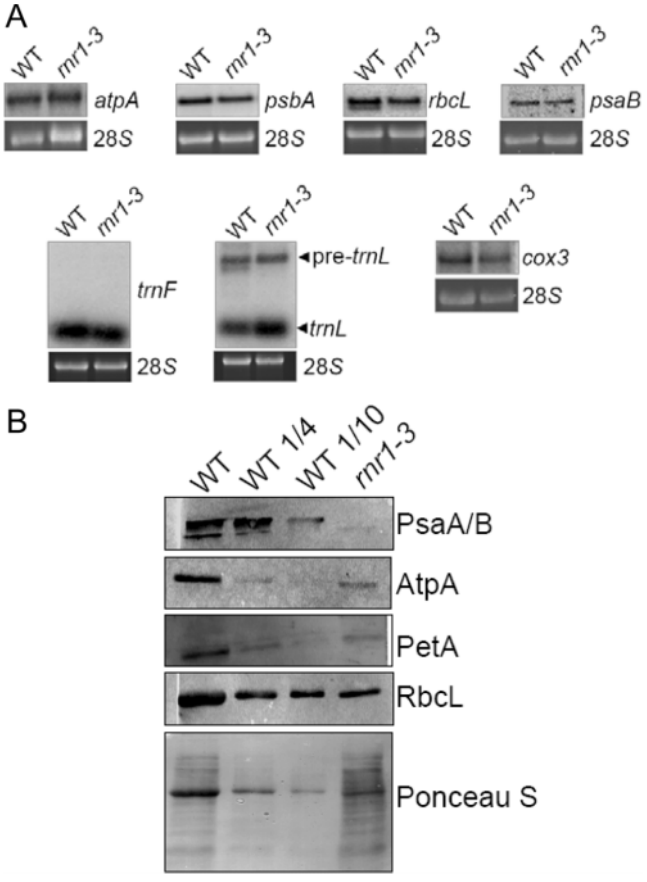

Figure 3. mRNA and protein accumulation in *rnr1* and WT plants. (**A**) One microgram of total RNA from WT or from *rnr1-3* was separated in a 1.2% agarose–formaldehyde gel and analyzed with the probes indicated to the right of each blot. 28S rRNA accumulation is shown in the ethidium bromide-stained membrane below each experiment to confirm equal loading. (**B**) Immunoblot analysis compares accumulation of the proteins shown at right in *rnr1* as compared with a dilution series of WT proteins. The stained filter is shown at the bottom as an estimate of gel loading.

accumulating WT levels of photosynthetic protein complexes. To test this hypothesis, total protein from WT or *rnr1* leaves was analyzed by immunoblotting (Figure 3B). Because accumulation of photosynthetic complex subunits is highly coordinated, changes in the accumulation of individual core subunits are indicative of the accumulation of the entire complex. Results of this analysis revealed that abundance of plastid-encoded subunits of the CF_0CF_1 ATPase complex (AtpA), the cytochrome b_6/f complex (PetA) and Rubisco (RbcL) decreased by at least 75% in the *rnr1* mutant, and that the accumulation of photosystem I (PsaA/B) was nearly undetectable. Since no defect in the accumulation of the cognizant mRNAs had been observed (Figure 3A) (data not shown), we tentatively concluded that *rnr1* mutants were defective in chloroplast translation.

RNR1 is important for rRNA accumulation

Because *rnr1* plants appeared to have a translation defect, the accumulation and processing of chloroplast rRNAs was analyzed (Figure 4). These rRNAs are encoded in a single operon that also encodes three tRNAs and is expressed as a 7.4 kb precursor RNA that is processed both endo- and exonucleolytically (Figure 4A) (11,24,25). Blots of total leaf RNA from WT or *rnr1* were probed as indicated in Figure 4B to test whether accumulation, processing or both were affected by the *rnr1* mutation.

When blots were probed for 16S rRNA (probe *A*), we found that WT leaves accumulated a mature 16S RNA transcript of 1.5 kb and low levels of a 1.7 kb precursor transcript that is generated by endonucleolytic cleavage in the 16S-tRNA^{Ile} intergenic space in the primary transcript, ~180 nt downstream of the mature 16S 3′ end (6). In contrast, *rnr1* plants accumulated 3-fold less mature 16S RNA than WT plants, and 3-fold more of the precursor. To positively identify the 1.7 kb RNA as the pre-16S RNA, blots were reanalyzed with probes derived from the intergenic spacer and flanking the endonucleolytic cleavage site (probes *B* and *C*). Probe *B* identified the 1.7 kb RNA, while probe *C* did not give a signal on these blots (data not shown), confirming that the longer transcript is the pre-16S RNA.

When RNA gel blots were analyzed with a 23S-specific probe (probe *D*), a complex pattern was revealed. 23S rRNA accumulates in chloroplasts as 7 major transcripts, the most noteworthy of which are the 1.2, 1.0 and 0.5 kb 23S* bands, which represent the mature 23S transcript after processing at 'hidden breaks' following incorporation into ribosomes (24), and a 3.2 kb band, which represents the 23S–4.5S dicistronic precursor RNA. There were no detectable differences in the sizes of these major 23S fragments, indicating that there were no apparent defects in 23S rRNA 3′ processing, in contrast to what was observed in chloroplast PNPase-deficient *Arabidopsis* (11). However, there were significant differences in the accumulation of several 23S RNA-containing transcripts. The 7.4 kb precursor RNA was visible in the *rnr1* plant, accumulation of the 3.2 kb 23S–4.5S dicistronic RNA increased 10-fold in *rnr1*, and accumulation of the 23S* fragments decreased 10-fold. A similar result was observed when blots were analyzed with a 4.5S probe (probe *E*): the dicistronic 23S–4.5S RNA over-accumulated in the mutant, and accumulation of the mature 0.1 kb 4.5S RNA decreased 10-fold.

When RNA gel blots were analyzed for the accumulation of 5S rRNA (probe *F*), we found that the accumulation of mature 5S rRNA (120 nt) was at least 10-fold lower in *rnr1* as compared with WT plants. Furthermore, mutant plants often accumulated low levels of an ~350 nt precursor 5S rRNA (pre-5S). The fact that RNR1 activity was previously implicated in 3′ exonucleolytic trimming of the mitochondrial *atp9* mRNA prompted a high-resolution analysis of chloroplast rRNA 3′ end processing.

RNR1 activity is essential for final rRNA 3′ end maturation

Because the size of 16S rRNA prevents the detection of small extensions by agarose gel blot analysis, its 5′ and 3′ ends were mapped by cRT–PCR (Figure 5). As expected, all 16S rRNA analyzed had mature 5′ and 3′ ends in WT plants (filled arrowheads). 16S rRNA 5′ ends were also processed correctly in *rnr1* plants, whereas no mature 16S 3′ ends were detected in the mutant plants (open arrowheads). Ten of eleven clones analyzed contained a 5 nt 3′ extension, and the remaining

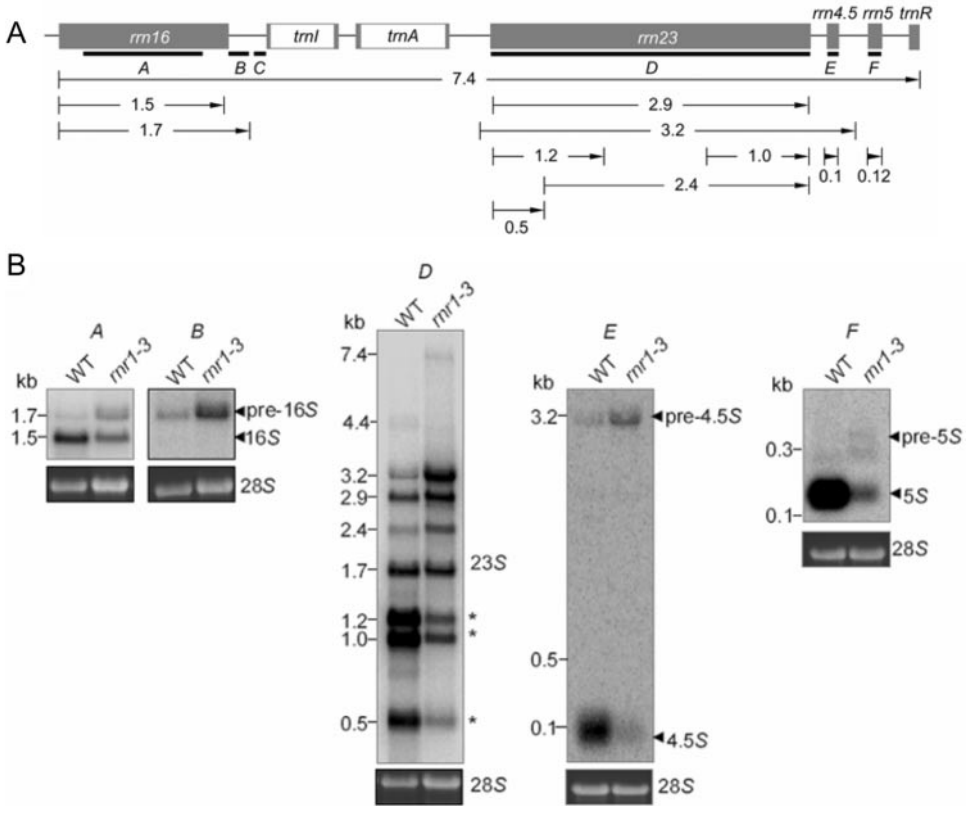

Figure 4. Analysis of rRNA expression and processing. (**A**) Diagram of the rRNA operon and location of probes (*A–F*) used for RNA gel blot analyses, and sizes of transcripts (in kb) observed by the gel blot analysis shown in (B). (**B**) RNA gel blot analysis. One microgram of total RNA from WT or *rnr1-3* was separated in 1.2% agarose–formaldehyde gels, and blots were probed as indicated above each blot, with transcripts identified shown to the right. 28S rRNA is shown in the ethidium bromide-stained membrane below each experiment to confirm equal loading. The transcripts marked by asterisks for probe *D* are mature 23S rRNA processed at hidden breaks (see text).

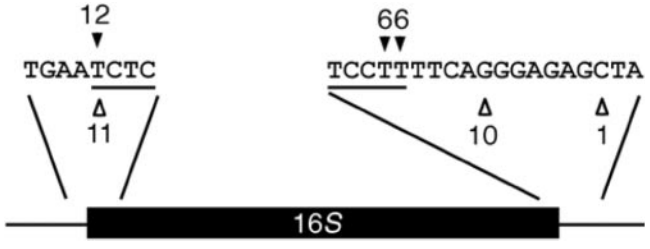

Figure 5. Mapping of 16S rRNA 5′ and 3′ ends by cRT–PCR. The 5′ and 3′ ends are shown by solid arrowheads for WT and by open arrowheads for *rnr1*, with numbers of corresponding clones obtained shown at each position. The 5′ and 3′ ends of the mature 16S rRNA sequence are underlined.

clone contained a 12 nt extension. Thus, while the lack of RNR1 causes only a modest increase in the accumulation of the 1.7 kb pre-16S RNA, the mutation prevents the final 3′ processing of the mature transcript.

The processing of 23S RNA at the hidden breaks complicates its analysis by cRT–PCR. Maturation of 23S 3′ ends was, therefore, analyzed by RNase protection, as shown in Figure 6. RNA from WT or from *rnr1* (or yeast tRNA as a negative control) was hybridized to a 190 nt antisense RNA probe (Figure 6A), digested with RNase T1 and RNase A, and analyzed in a 6% denaturing polyacrylamide gel (Figure 6B). In RNA samples from WT plants, the probe protected an 86 nt fragment that represents the mature 23S RNA and, to a lesser extent, an ∼184 nt band that represents the dicistronic 23S–4.5S species, as shown below. No mature 23S 3′ ends were observed in the *rnr1* mutant, but these plants did accumulate incompletely processed 23S 3′ ends with 10–15 nt extensions. Thus, 3′ end maturation of both 16S and 23S rRNAs is affected in *rnr1*.

The small sizes of 4.5S and 5S rRNAs allow their analysis by high-resolution RNA gel blots in addition to RNase protection. As shown in Figure 7A, although monocistronic 4.5S rRNA accumulates to a much lower level in *rnr1* plants than in WT, no defect in its 3′ processing was observed, which would have been apparent as a slightly longer species. The 3′ end processing of 4.5S rRNA was also analyzed by RNase protection (Figure 7B and C). In WT plants, 4.5S rRNA accumulates both as a mature species of ∼97–99 nt, and as a weaker band of ∼270 nt, which represents an ∼170 nt 3′ extension. In the mutant, a significantly higher proportion of 4.5S rRNA accumulated as the precursor species, but a low level of mature 4.5S rRNA also accumulated, as was observed by RNA gel blot.

While RNase protection clearly showed the accumulation of precursor 4.5S transcripts in the mutant (Figure 7C), RNA gel blot analysis suggested that these did not represent monocistronic pre-4.5S rRNAs, as such a species of ∼270 nt would have easily been observed (Figure 4B, probe *E*; Figure 7A). It was likely, therefore, that the 4.5S precursors were derived entirely from dicistronic 23S–4.5S species rather than from

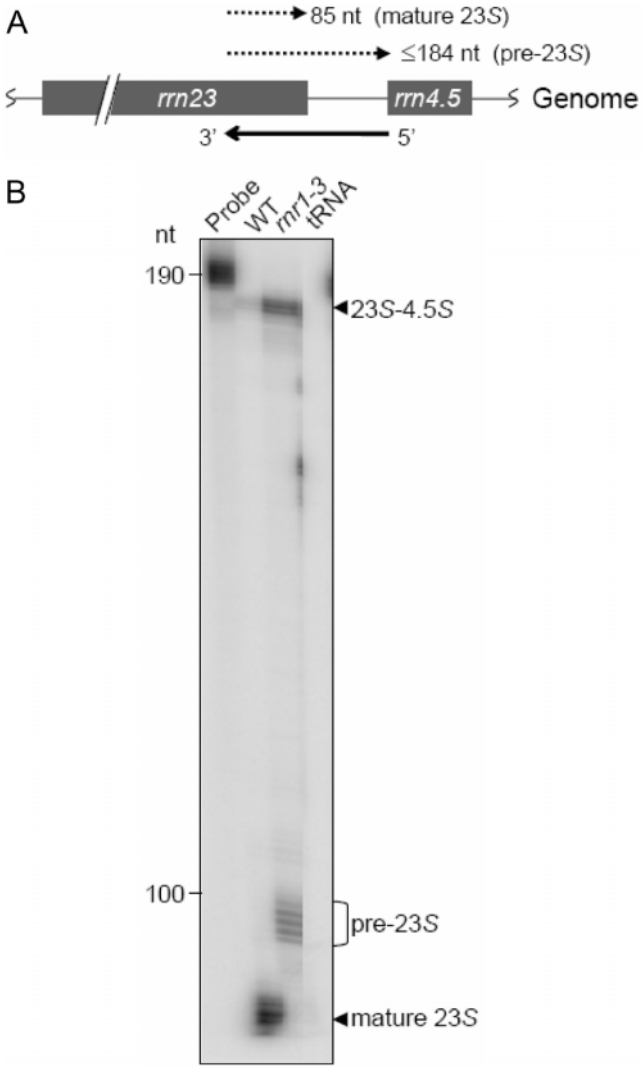

Figure 6. Analysis of 23S 3′ end processing by RNase protection. (**A**) The probe is indicated below the diagram of the 4.5S–5S region of the rrn operon. Sizes of protected RNAs found in (B) are indicated above the schematic. (**B**) Protected RNA from WT or from *rnr1-3*, as indicated above each lane, was separated in a 6% denaturing polyacrylamide gel. The positions of protected bands corresponding to mature and pre-23S RNAs are indicated at right, and size standards are at left.

moncistronic pre-4.5S transcripts. Significant accumulation of both the 4.5S rRNA precursor and the 23S–4.5S transcripts is consistent with the view that processing of the 4.5S rRNA 3′ end is a prerequisite to its cleavage from 23S rRNA, as has been previously suggested (4). This was tested by probing an RNA gel blot either with a 4.5S-specific oligonucleotide as a control (Figure 8A, left panel) or with a 4.5S rRNA precursor-specific oligonucleotide (Figure 8A, right panel). While the 4.5S-specific probe detected both dicistronic and mature 4.5S transcripts as expected, the precursor-specific probe detected only the dicistronic RNA, and not an ~270 nt species.

To better characterize the 23S–4.5S species, both 5′ and 3′ ends of this precursor were mapped by cRT–PCR. Two types of 5′ ends were detected, both in WT and in *rnr1* plants, and coincided either with the annotated mature 23S 5′ end or to a position 72–73 nt upstream (Figure 8B). As expected, more clones corresponding to the mature 5′ ends were detected in WT than in *rnr1*, but the lack of RNR1 did not seem to influence the location of these maturation sites. Interestingly, the 8 and 3 clones in WT and *rnr1*, respectively, which had mature 23S RNA 5′ ends, also had mature 4.5S rRNA 3′ ends (Figure 8C). This would represent the mature dicistronic intermediate prior to endonucleolytic cleavage between 23S and 4.5S rRNAs. However, due to the use of T4 RNA ligase during cRT–PCR it is not possible to exclude the ligation of mature 23S and mature 4.5S prior to cDNA synthesis. Nevertheless, all clones with unprocessed 23S rRNA 5′ ends also had unprocessed 4.5S rRNA 3′ ends, both in WT and in *rnr1* (Figure 8C). Although the 3′ ends of two clones from the mutant mapped downstream of the 5S rRNA, representing the 23S–4.5S–5S processing intermediate, most 3′ ends of 23S–4.5S precursors mapped to a cluster of 4 nt situated 170 nt downstream of the 4.5S rRNA, as predicted by RNase protection (Figure 7C). This region likely represents an endonucleolytic cleavage site between the 4.5S and 5S rRNAs.

Both RNA gel blot and cRT–PCR data suggested that 3′ maturation of 4.5S rRNA precedes or occurs concomitantly with endonucleolytic cleavage of the dicistronic 23S–4.5S rRNA and, furthermore, that the impaired endonucleolytic processing of the 23S–4.5S dicistronic species in *rnr1* plants is a pleiotropic effect of the lack of RNR1. Although it is tempting to suggest that incomplete 4.5S rRNA 3′ processing is a primary defect of RNR1 deficiency, there is no direct evidence that this is the case, and accumulation of the 23S–4.5S species has been observed in unrelated chloroplast biogenesis mutants (2,6,8).

To study the involvement of RNR1 in 5S rRNA 3′ end processing more closely, both RNase protection and cRT–PCR experiments were performed. Figure 9B shows that a 5S antisense probe (Figure 9A) protected mature 5S rRNA from both WT and *rnr1* plants, whereas *rnr1* mutants alone accumulated a population of 5S precursor RNAs with short, heterogeneous 3′ extensions averaging 10 nt in length, as well as a full-length precursor of 351 nt, which is most likely generated by RNase P cleavage at the 5′ end of $tRNA^{Arg}$, and which was previously observed by agarose RNA gel blot analysis (Figure 4B, probe *F*). cRT–PCR was used to reveal the precise 3′ ends of the pre-5S rRNAs. As shown in Figure 9C, all the clones obtained from WT RNA contained mature 5′ and 3′ ends, and although a few such clones were also obtained from *rnr1* plants, most clones from the mutant contained small 3′ extensions ranging from 1 to 11 nt. Together, these data indicate that RNR1 is involved in trimming these extensions, although since a small proportion of 5S rRNA mature 3′ ends was observed, they can also be apparently generated by an RNR1-independent route.

Purified RNR1 accurately processes pre-5S rRNA *in vitro*

C-terminal-tagged RNR1 (RNR1-tag) was purified from a transgenic overexpressing line to check whether RNR1 was able to perform *in vitro* the 3′ processing of 5S rRNA (Figure 10). A mock purification was also performed from plants that did not overexpress tagged RNR1. Both fractions were incubated with RNA substrates corresponding to mature 5S rRNA, or to a precursor 5S rRNA containing a 20 nt

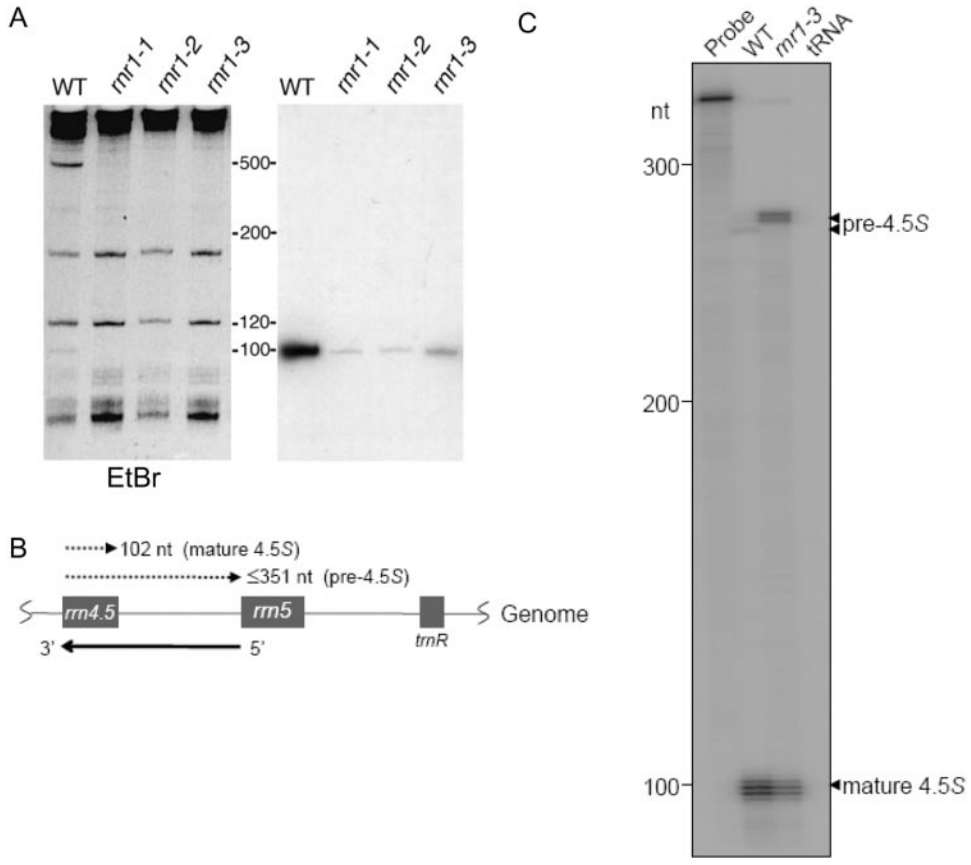

Figure 7. Analysis of 4.5S and 3′ end processing. (**A**) An aliquot of 1.5 μg of total RNA from WT, *rnr1-1*, *rnr1-2* and *rnr1-3* was separated on a 12% acrylamide gel and stained with ethidium bromide (left panel) or analyzed with a 4.5S rRNA-specific probe (right panel). Migration and size (nt) of molecular weight markers are indicated. (**B**) The probe used in this analysis is indicated by the heavy arrow below the schematic of the 4.5S–5S–tRNA^{Arg} region of the *rrn* operon. Sizes of protected RNAs seen in (C) are indicated above the schematic. (**C**) Protected RNA from WT or from *rnr1-3*, as indicated above each lane, was separated in a 6% denaturing polyacrylamide gel. The positions of protected bands corresponding to mature and pre-4.5S rRNAs are indicated at right, and size standards are at left.

3′ extension (5S and 5S + 20, respectively, Figure 10). No RNase activity was observed with the mock fraction or in buffer alone, but tagged RNR1 efficiently digested the 20 nt extension to generate a mature 5S rRNA 3′ end. These data confirm the results obtained in *rnr1* plants, i.e. RNR1 can trim the 3′ ends of 5S rRNA precursors.

Polysome association of mRNAs decreases in rnr1 chloroplasts

Because *rnr1* plants contained significantly fewer mature ribosomal RNAs than WT plants, and because the mutants accumulated lower levels of chloroplast-encoded proteins, the association of chloroplast mRNAs with ribosomes was examined, as shown in Figure 11. Extracts from WT or *rnr1* leaves were sedimented through 15–55% sucrose density gradients and following centrifugation, fractions were collected and analyzed by RNA gel blot with the probes indicated in the right margin. As judged by the levels of 23S* and mature 16S transcripts in polysomal fractions (∼8–12), *rnr1* chloroplasts contain significantly fewer polysomes than WT chloroplasts.

Polysome loading of mRNAs was differentially affected in *rnr1* plants. The transcript encoding the *psaA-psaB-rps14* transcript was shifted toward the top of the gradient, indicating that it was associated with fewer ribosomes in *rnr1* than in WT plants. These results would presumably correlate with lower protein synthesis rates, although we did not measure protein synthesis directly. The *rbcL*, *psbA* and *atpB*/*E* transcripts, however, showed a similar pattern in WT and in *rnr1*, suggesting that these transcripts were being loaded under conditions where ribosomes might be limiting for translation.

DISCUSSION

RNR1 is a ubiquitous, dual-targeted exoribonuclease that is important for chloroplast rRNA processing. Here, we have presented a detailed analysis of *rnr1* null mutants, which has illuminated several facets of chloroplast rRNA maturation. The RNA phenotypes presented here are much more striking than those observed in mitochondria of one of the same null mutant lines, *rnr1-2* (14), raising the question of whether RNR1 is a minor player in mitochondria. Just as perplexing are the contradictory GFP targeting results which, rather than showing dual targeting in any of three laboratories which tested similar fusions [(14,15) and Supplementary Figure 1], generated either uniquely chloroplast or uniquely mitochondrial targeting. While the fusions made in each case were slightly different and GFP is well-known to produce artifacts, such results are unusual but not unprecedented (26). Furthermore, short nucleotide extensions were found in both

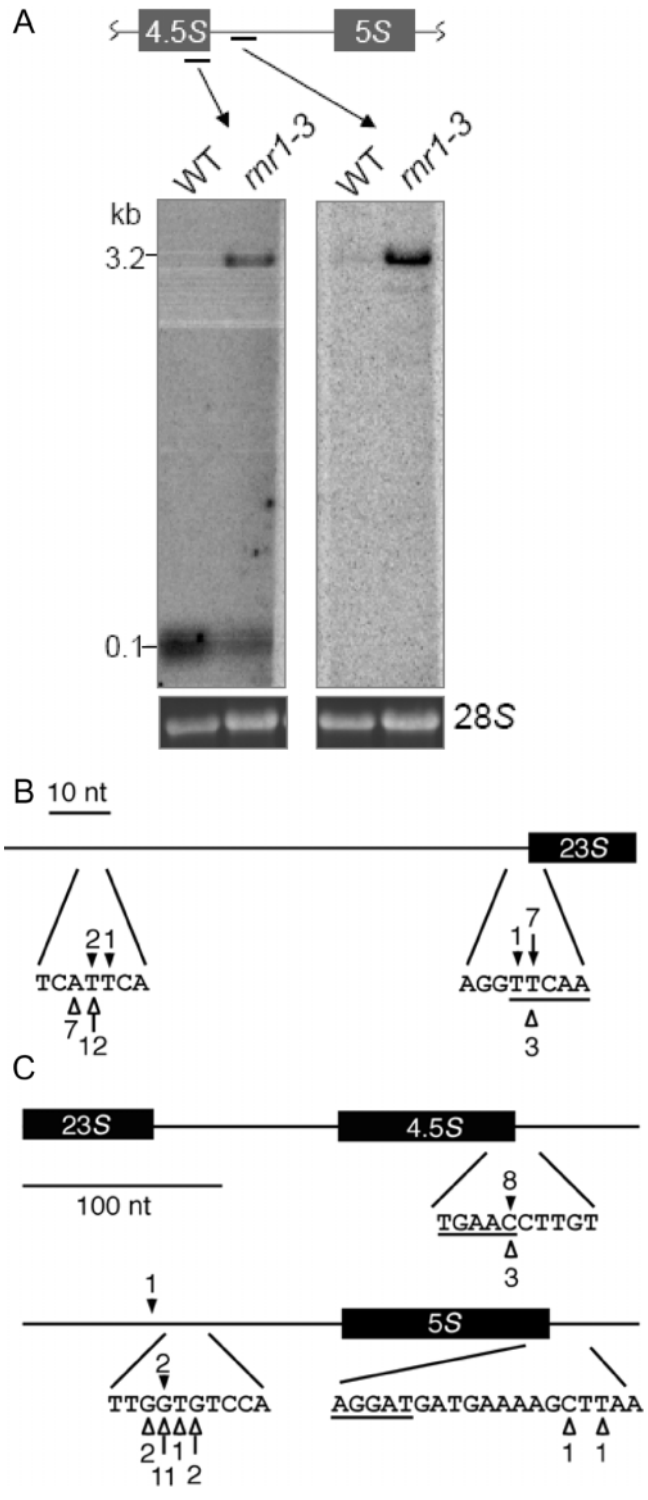

Figure 8. Ordered processing of the 23S–4.5S rRNA. (**A**) Analysis of 4.5S precursor rRNA accumulation. One microgram of total RNA from either WT or from *rnr1-3* was separated in a 1.2% agarose–formaldehyde gel, and probed with the oligonucleotides indicated in the diagram above. 28S rRNA accumulation on the ethidium bromide-stained membrane is shown below each blot to confirm equal loading. (**B**) Mapping 23S–4.5S precursor 5′ ends by cRT–PCR. The 5′ ends are shown by solid arrowheads for WT and by open arrowheads for *rnr1*, with numbers of corresponding clones obtained shown at each position. The 5′ end of the mature 23S rRNA is underlined. (**C**) Mapping of 23S–4.5S precursor 3′ ends by cRT–PCR, labeled as in (B). The mature 4.5S and 5S rRNA 3′ ends are underlined.

organelles in *rnr1* plants, suggesting that indeed RNR1 is present both in mitochondria and in chloroplasts. In the longer term, careful immunoblot analysis should resolve these remaining ambiguities.

Chloroplast 23S rRNA maturation requires several processing steps

Chloroplast rrn operon processing differs somewhat from that of *Escherichia coli*. In *E.coli*, 16S and 23S precursor RNAs are excised from a 30S precursor by RNase III, which cleaves the double-stranded stem formed by base pairing of their 5′ and 3′ ends. This is followed by endonucleolytic 5′ end maturation by RNase E, which for 23S RNA generates a 3′ overhang that is subsequently processed exonucleolytically to the mature 3′ end by RNase T, and to some extent by RNase PH (27). The 3′ end processing of 23S RNA occurs on the ribosome, as RNase T-deficient cells accumulate ribosomes with immature 23S RNA (27).

Based on its homologous position in the rrn operon, chloroplast 4.5S rRNA is derived from the fragmentation of the 23S rRNA (28,29), which is accompanied by a 99 nt insertion in *Arabidopsis*. Endonucleolytic processing within this sequence results in the formation of a mature 4.5S rRNA and a slightly shorter 23S RNA, in comparison with those of most bacteria (29). Therefore, *E.coli* 23S RNA 3′ processing can be compared with chloroplast 23S–4.5S rRNA 3′ processing.

In chloroplasts, there is no sequence complementarity between the 23S 5′ end and the 4.5S rRNA 3′ end that would suggest base pairing and endonucleolytic excision from the 7.4 kb precursor by an endonuclease like RNase III. In contrast, the 23S–4.5S intermediate is generated by endonucleolytic cleavage ∼78 nt upstream of the mature 23S 5′ end, and ∼170 nt downstream of the 4.5S rRNA 3′ end. This is followed by 3′ maturation of the 4.5S sequence in a single step, which either precedes or occurs concomitantly with 23S 5′ processing, since cRT–PCR has shown that dicistronic intermediates with mature 4.5S rRNA 3′ ends also have mature 23S 5′ ends. Our data are also consistent with the hypothesis that 4.5S rRNA 3′ maturation must precede excision of the 4.5S rRNA from the dicistronic intermediate (3,4). This is reminiscent of the ordered mitochondrial tRNA processing, although in those cases 3′ end maturation is dependent on 5′ maturation (30,31).

The 5′ end maturation of 23S rRNA is probably endonucleolytic, as there is no evidence for a 5′–3′ exoribonuclease in plant chloroplasts (32), although ample evidence for this activity exists for *Chlamydomonas* chloroplasts (33,34). Based on sedimentation of the dicistronic intermediate with polysomes in sucrose density gradients, this processing occurs on ribosomes, as has been proposed previously for the *Brassica napus* 23S–4.5S intermediate and for *E.coli* 23S rRNA (4,35,36).

Maturation of the 4.5S rRNA 3′ end

Processing of the 4.5S rRNA 3′ end occurs in a single step, and based on polysome analysis, both this and final maturation of 23S rRNA also occur on ribosomes. In *rnr1* mutants, accumulation of translation-competent ribosomes is limited, presumably due to limiting levels of mature 16S or 5S rRNA or both. This is also thought to be true of maize *hcf7* and

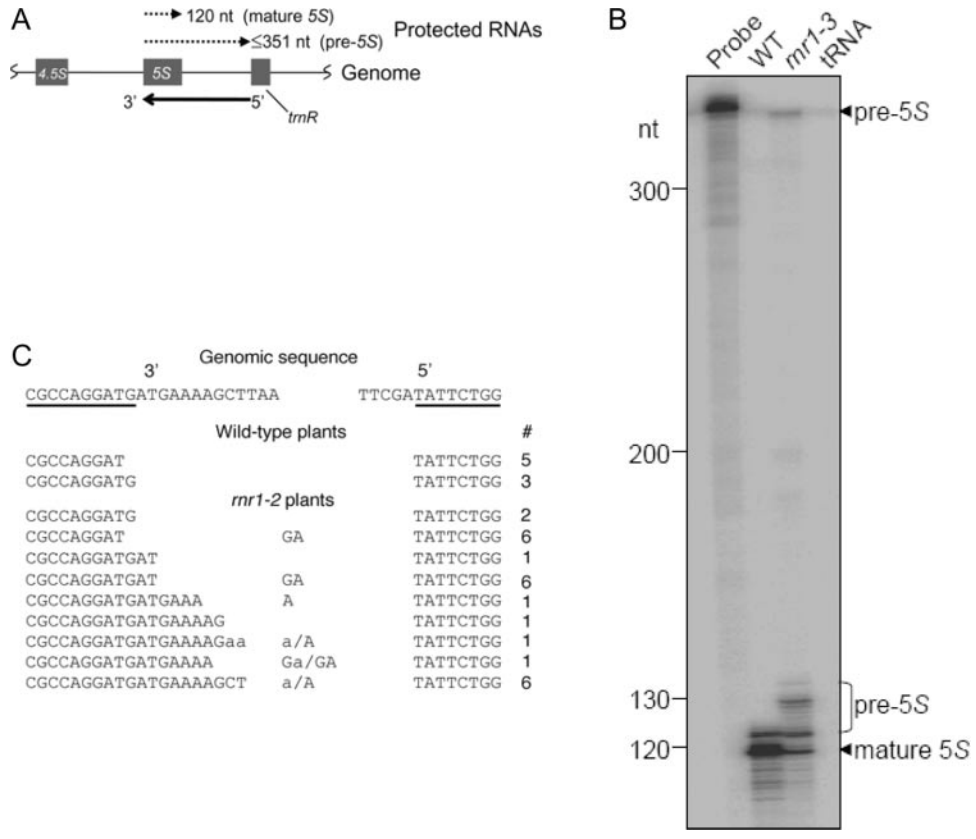

Figure 9. Analysis of 5S rRNA 3′ end processing. (**A**) The probe is indicated by the heavy arrow below the diagram of the 4.5S–5S–tRNA^{Arg} region. Sizes of protected RNAs seen in (C) are indicated above the diagram. (**B**) Protected RNA from WT or from *rnr1-3*, as indicated above each lane, was separated in a 6% denaturing polyacrylamide gel. The positions of protected bands corresponding to mature and pre-5S rRNAs are indicated at the right, and size standards are at the left. (**C**) Mapping of 5S rRNA 5′ and 3′ ends by cRT–PCR. The genomic sequence is shown at the top, with the mature 3′ and 5′ ends underlined. 5S rRNA 3′ and 5′ ends obtained for WT and *rnr1* plants are indicated with the number on the right representing the number of clones for each sequence. Nucleotides that could be present either at 3′ or at 5′ ends are indicated in the middle column. Adenosines that are added post-transcriptionally are in lowercase.

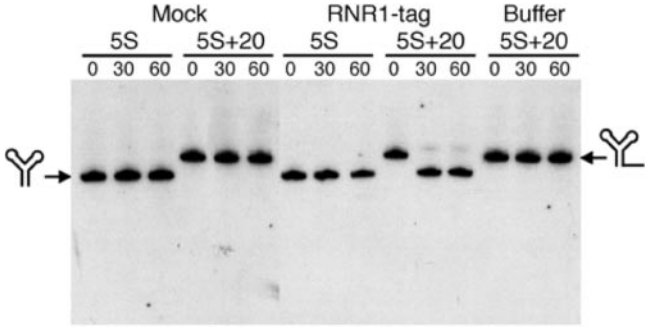

Figure 10. RNR1 accurately processes 5S rRNA 3′ ends *in vitro*. Affinity-purified RNR1-tag and a fraction from a mock purification were incubated with substrates corresponding to the mature 5S rRNA (5S) or to the same RNA with a 20 nt 3′ extension (5S + 20). Incubation times are indicated in minutes above each lane and the positions and putative secondary structures of substrate and product are indicated at the right and left, respectively.

Arabidopsis dal1-2 (5,6), which are impaired in pre-16S 3′ end maturation. Both *dal1-2* and the tomato *dcl-s* mutant, which is defective in an unidentified step of ribosome assembly, accumulate abnormal levels of the 23S–4.5S processing intermediate (2,6). Therefore, in *rnr1* mutants, the 23S–4.5S intermediate may accumulate simply because ribosome assembly is slowed and its accumulation may, therefore, be a pleiotropic effect of the mutation. Because some mature 4.5S and 23S rRNAs accumulate and because *rnr1* chloroplasts are clearly not entirely bereft of translation, an RNR1-independent pathway for ribosome maturation, perhaps relying on PNPase, must operate in the mutant.

23S 3′ end maturation is catalyzed by PNPase and by RNR1

Similar to plant chloroplasts, many eubacterial species encode a fragmented 23S rRNA, whose intervening sequences (IVSs) are removed by looping out and RNase III-directed cleavage of the intergenic spacer (37). In contrast, once incorporated into ribosomes, chloroplast 23S–4.5S rRNA processing includes an endonucleolytic cleavage to produce the monocistronic 4.5S rRNA and a 23S precursor rRNA, and two subsequent exonucleolytic events, PNPase-catalyzed generation of a precursor with 10–15 nt extensions (11), followed by RNR1 trimming. Removal of the pre-23S 3′ extension is not required for ribosome assembly and translation (11), which is also true of S*almonella typhimurium* 23S IVS processing (38–40). Because defects in 23S RNA IVS processing are phenotypically silent, their physiological significance is unknown.

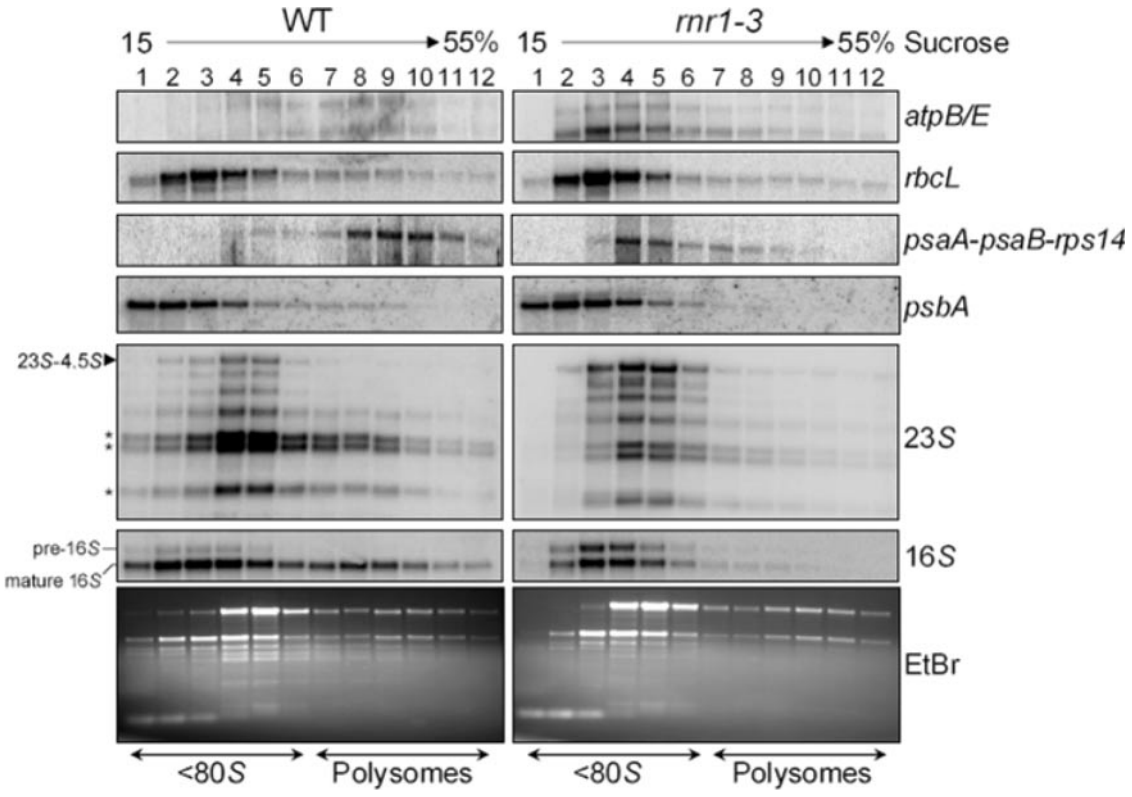

Figure 11. Sucrose density gradient fractions from WT and *rnr1* were analyzed by RNA gel blot with the probes indicated to the right of each panel. The 12 lanes from left to right indicate the gradient fractions, with 1 representing the top of the gradient and 12 representing the bottom of the gradient. An ethidium bromide-stained membrane for each sample is included; equal proportions of each fraction were loaded. The positions of ribosomal (<80S) and polysomal fractions were determined by running puromycin-treated samples in parallel to experimental samples, as indicated at the bottom.

Chloroplast 5S rRNA maturation requires two exonucleolytic processing steps

5S rRNA maturation pathways vary widely, even among bacteria. In *E.coli*, the 9S precursor is cleaved 3 nt upstream of the 5S rRNA 5′ end and 3 nt downstream of its 3′ end by RNase E (41), incorporated into ribosomes, and its 3′ end is trimmed primarily by RNase T (42). However, not all organisms require RNase E for rRNA processing. *Bacillus subtilis* and many other gram-positive bacteria generate mature 5S rRNA directly by double-stranded cleavage of the 5S 'molecular stalk' by RNase M5 (43,44). The *Arabidopsis* nuclear genome encodes an RNase E-like protein that is predicted to be chloroplast targeted (At2g04270), but whether this enzyme is important in rRNA processing is unknown.

As in *E.coli*, chloroplast 5S rRNA appears to be generated by single-stranded endonucleolytic cleavages upstream and downstream of the mature 5S sequence, although the precursor is much longer. Based on our results, the chloroplast pre-5S rRNA 3′ end is generated by endonucleolytic cleavage near the 5′ end of $tRNA^{Arg}$, possibly by RNase P, to generate the 350 nt precursor sometimes observed in *rnr1* plants. This precursor is trimmed through sequential exonucleolytic steps, the first generating transcripts with 10–15 nt 3′ extensions, and the second generating the mature 3′ end. One or both of these steps appear to be catalyzed by RNR1, but because some mature 5S rRNA accumulates in *rnr1* mutants, another less active exonuclease, perhaps PNPase, can act in its place.

An interesting observation is that while 16S, 23S and 23S–4.5S precursors accumulated significantly in *rnr1*, the 350 nt 5S rRNA precursor did not, and was often difficult to observe. We hypothesize, therefore, that it is actively degraded, possibly through the polyadenylation-dependent RNA turnover pathway. Polyadenylation of pre-5S rRNA in an *E.coli* RNase $T^-PH^-D^-BN^-$ mutant strain has been observed previously (45).

RNR1 may require accessory proteins for processivity *in vivo*

Similar to purified *E.coli* RNase II and RNase R, recombinant RNR1 is a non-specific exoribonuclease. The question, then, is what drives RNRs1 substrate specificity *in vivo*. One probability is that RNR1 activity, similar to that of *E.coli* RNase II (46), is modulated by RNA secondary structure *in vivo*, much as it is *in vitro* (14,19). Secondary structure increases the stability of mRNAs, such as the *trpT* terminator, and in general those containing repetitive extragenic palindrome sequences in bacteria (47–49), or 3′ stem–loop structures in chloroplasts (1). In this view, RNR1 would digest the unstructured extensions downstream of the mature rRNA 3′ ends, but stall when it reached their structured regions. The specificity of RNR1 in rRNA processing is also emphasized by the fact that the maturation of *trnR* appeared to be RNR1-independent, or the role of RNR1 is fully redundant in its processing.

However, *rnr1* mutants were less efficient at processing long, highly structured pre-16S, pre-23S–4.5S and to a lesser

extent, pre-5S transcripts. Therefore, we cannot exclude that RNR1 could be partially responsible for processing these tails. This facet of RNR1 activity might require accessory protein(s). By analogy to the *E.coli* degradosome, where the association of PNPase with the RNA helicase RhlB allows it to turn over highly structured substrates (50,51), it is possible that RNR1 processivity is enhanced by its association with an RNA helicase. One candidate is the chloroplast RNA helicase encoded by *VDL* (52), which is essential for the function of all plastid types, as would be expected of an rRNA maturation factor. Whether the *vdl* mutant accumulates aberrant plastid transcripts remains to be reported.

Arabidopsis contains three RNR genes

Residual rRNA processing in *rnr1* prompted us to search for additional members of the RNR superfamily encoded in the *Arabidopsis* nuclear genome, and two such genes were found. We have tentatively designated these *RNR2* (At1g77680) and *RNR3* (At2g17510). While experiments with the RNR N-terminal 100 amino acids fused to GFP confirmed chloroplast targeting for RNR1, the putative RNR2 transit peptide (N-terminal 231 amino acid) targeted GFP to the nucleus and RNR3 targeting, using the N-terminal 194 amino acid of RNR3, resembled that of the untagged GFP control, suggesting that RNR2 and RNR3 might be components of the exosome (Supplementary Figure 1) (23). Therefore, chloroplasts appear to contain only a single RNR family enzyme, as well as PNPase. Whether these enzymes catalyze redundant activities remains to be seen, but a *pnp1*/*rnr1* double mutant is embryo lethal (S. Yehudai-Resheff, T. Bollenbach, R. Gutierrez and D. Stern, manuscript in preparation).

SUPPLEMENTARY MATERIAL

Supplementary Material is available at NAR Online.

ACKNOWLEDGEMENTS

The authors thank the Salk Institute Genomic Analysis Laboratory for providing the sequence-indexed *Arabidopsis* T-DNA insertion mutants. This work was supported by DOE Energy Biosciences Program award DE-FG02-90ER20015 to D.B.S., an EMBO long-term fellowship to H.L. and an ACI JC grant from the French ministry of research to D.G. and the Centre National de la Recherche Scientifique (CNRS, France). Funding to pay the Open Access publication charges for this article was provided by the DOE Energy Biosciences Program.

Conflict of interest statement. None declared.

REFERENCES

1. Monde,R.A., Schuster,G. and Stern,D.B. (2000) Processing and degradation of chloroplast mRNA. *Biochimie*, **82**, 573–582.
2. Bellaoui,M., Keddie,J.S. and Gruissem,W. (2003) *DCL* is a plant-specific protein required for plastid ribosomal RNA processing and embryo development. *Plant Mol. Biol.*, **53**, 531–543.
3. Keus,R.J.A., Dekker,A.F., Kreuk,K.C.J. and Groot,G.S.P. (1984) Transcription of ribosomal DNA in chloroplasts of S*pirodela oligorhiza*. *Curr. Genet.*, **9**, 91–98.
4. Leal-Klevezas,D.S., Martinez-Soriano,J.P. and Nazar,R.N. (2000) Transcription and processing map of the 4.5S–5S rRNA intergenic region (ITS3) from rapeseed (*Brassica napus*) chloroplasts. *Plant Cell Rep.*, **19**, 667–673.
5. Barkan,A. (1993) Nuclear mutants of maize with defects in chloroplast polysome assembly have altered chloroplast RNA metabolism. *Plant Cell*, **5**, 389–402.
6. Bisanz,C., Begot,L., Carol,P., Perez,P., Bligny,M., Pesey,H., Gallois,J.L., Lerbs-Mache,S. and Mache,R. (2003) The *Arabidopsis* nuclear *DAL* gene encodes a chloroplast protein which is required for the maturation of the plastid ribosomal RNAs and is essential for chloroplast differentiation. *Plant Mol. Biol.*, **51**, 651–663.
7. Yamamoto,Y.Y., Puente,P. and Deng,X.W. (2000) An *Arabidopsis* cotyledon-specific albino locus: a possible role in 16S rRNA maturation. *Plant Cell Physiol.*, **41**, 68–76.
8. Bellaoui,M. and Gruissem,W. (2004) Altered expression of the *Arabidopsis* ortholog of *DCL* affects normal plant development. *Planta*, **219**, 819–826.
9. Schultes,N.P., Sawers,R.J., Brutnell,T.P. and Krueger,R.W. (2000) Maize high chlorophyll fluorescent 60 mutation is caused by an Ac disruption of the gene encoding the chloroplast ribosomal small subunit protein 17. *Plant J.*, **21**, 317–327.
10. Pesaresi,P., Varotto,C., Meurer,J., Jahns,P., Salamini,F. and Leister,D. (2001) Knock-out of the plastid ribosomal protein L11 in *Arabidopsis*: effects on mRNA translation and photosynthesis. *Plant J.*, **27**, 179–189.
11. Walter,M., Kilian,J. and Kudla,J. (2002) PNPase activity determines the efficiency of mRNA 3′-end processing, the degradation of tRNA and the extent of polyadenylation in chloroplasts. *EMBO J.*, **21**, 6905–6914.
12. Cheng,Z.F. and Deutscher,M.P. (2005) An important role for RNase R in mRNA decay. *Mol. Cell*, **17**, 313–318.
13. Cheng,Z.F. and Deutscher,M.P. (2003) Quality control of ribosomal RNA mediated by polynucleotide phosphorylase and RNase R. *Proc. Natl Acad. Sci. USA*, **100**, 6388–6393.
14. Perrin,R., Meyer,E.H., Zaepfel,M., Kim,Y.J., Mache,R., Grienenberger,J.M., Gualberto,J.M. and Gagliardi,D. (2004) Two exoribonucleases act sequentially to process mature 3′-ends of *atp9* mRNAs in *Arabidopsis* mitochondria. *J. Biol. Chem.*, **279**, 25440–25446.
15. Kishine,M., Takabayashi,A., Munekage,Y., Shikanai,T., Endo,T. and Sato,F. (2004) Ribosomal RNA processing and an RNase R family member in chloroplasts of *Arabidopsis*. *Plant Mol. Biol.*, **55**, 595–606.
16. Alonso,J.M., Stepanova,A.N., Leisse,T.J., Kim,C.J., Chen,H., Shinn,P., Stevenson,D.K., Zimmerman,J., Barajas,P., Cheuk,R. *et al.* (2003) Genome-wide insertional mutagenesis of *Arabidopsis thaliana*. *Science*, **301**, 653–657.
17. Murashige,T. and Skoog,F. (1962) A revised medium for rapid growth and bioassays with tobacco tissue cultures. *Physiol. Plant*, **15**, 473–497.
18. Church,G. and Gilbert,W. (1984) Genomic sequencing. *Proc. Natl Acad. Sci. USA*, **81**, 1991–1995.
19. Perrin,R., Lange,H., Grienenberger,J.M. and Gagliardi,D. (2004) AtmtPNPase is required for multiple aspects of the 18S rRNA metabolism in *Arabidopsis thaliana* mitochondria. *Nucleic Acids Res.*, **32**, 5174–5182.
20. Barkan,A. (1998) Approaches to investigating nuclear genes that function in chloroplast biogenesis in land plants. *Methods Enzymol.*, **297**, 38–57.
21. Stern,D.B. and Gruissem,W. (1987) Control of plastid gene expression: 3′ inverted repeats act as mRNA processing and stabilizing elements, but do not terminate transcription. *Cell*, **51**, 1145–1157.
22. Monde,R.A., Greene,J.C. and Stern,D.B. (2000) Disruption of the *petB–petD* intergenic region in tobacco chloroplasts affects *petD* RNA accumulation and translation. *Mol. Gen. Genet.*, **263**, 610–618.
23. Zuo,Y. and Deutscher,M.P. (2001) Exoribonuclease superfamilies: structural analysis and phylogenetic distribution. *Nucleic Acids Res.*, **29**, 1017–1026.
24. Strittmatter,G. and Kossel,H. (1984) Cotranscription and processing of 23S, 4.5S and 5S rRNA in chloroplasts from *Zea mays*. *Nucleic Acids Res.*, **12**, 7633–7647.
25. Leal-Klevezas,D.S., Martinez-Soriano,J.P. and Nazar,R.N. (2000) Cotranscription of 5S rRNA–tRNA(Arg)(ACG) from *Brassica napus* chloroplasts and processing of their intergenic spacer. *Gene*, **253**, 303–311.
26. Beardslee,T.A., Roy-Chowdhury,S., Jaiswal,P., Buhot,L., Lerbs-Mache,S., Stern,D.B. and Allison,L.A. (2002) A nucleus-encoded maize protein with sigma factor activity accumulates in mitochondria and chloroplasts. *Plant J.*, **31**, 199–209.
27. Li,Z., Pandit,S. and Deutscher,M.P. (1999) Maturation of 23S ribosomal RNA requires the exoribonuclease RNase T. *RNA*, **5**, 139–146.

28. Bowman,C.M. and Dyer,T.A. (1979) 4.5S ribonucleic acid, a novel ribosome component in the chloroplasts of flowering plants. *Biochem. J.*, **183**, 605–613.
29. Edwards,K. and Kossel,H. (1981) The rRNA operon from *Zea mays* chloroplasts: nucleotide sequence of 23S rDNA and its homology with *E.coli* 23S rDNA. *Nucleic Acids Res.*, **9**, 2853–2869.
30. Kunzmann,A., Brennicke,A. and Marchfelder,A. (1998) 5′ end maturation and RNA editing have to precede tRNA 3′ processing in plant mitochondria. *Proc. Natl Acad. Sci. USA*, **95**, 108–113.
31. Wang,M.J., Davis,N.W. and Gegenheimer,P. (1988) Novel mechanisms for maturation of chloroplast transfer RNA precursors. *EMBO J.*, **7**, 1567–1574.
32. Bollenbach,T.J., Schuster,G. and Stern,D.B. (2004) Cooperation of endo- and exoribonucleases in chloroplast mRNA turnover. *Prog. Nucleic Acid Res. Mol. Biol.*, **78**, 305–337.
33. Drager,R.G., Girard-Bascou,J., Choquet,Y., Kindle,K.L. and Stern,D.B. (1998) *In vivo* evidence for 5′3′ exoribonuclease degradation of an unstable chloroplast mRNA. *Plant J.*, **13**, 85–96.
34. Vaistij,F.E., Goldschmidt-Clermont,M., Wostrikoff,K. and Rochaix,J.D. (2000) Stability determinants in the chloroplast *psbB/T/H* mRNAs of *Chlamydomonas reinhardtii*. *Plant J.*, **21**, 469–482.
35. Sirdeshmukh,R. and Schlessinger,D. (1985) Why is processing of 23S ribosomal RNA in *Escherichia coli* not obligate for its function? *J. Mol. Biol.*, **186**, 669–672.
36. Sirdeshmukh,R. and Schlessinger,D. (1985) Ordered processing of *Escherichia coli* 23S rRNA *in vitro*. *Nucleic Acids Res.*, **13**, 5041–5054.
37. Burgin,A.B., Parodos,K., Lane,D.J. and Pace,N.R. (1990) The excision of intervening sequences from S*almonella* 23S ribosomal RNA. *Cell*, **60**, 405–414.
38. Mattatall,N.R. and Sanderson,K.E. (1998) RNase III deficient S*almonella typhimurium* LT2 contains intervening sequences (IVSs) in its 23S rRNA. *FEMS Microbiol. Lett.*, **159**, 179–185.
39. Kordes,E., Jock,S., Fritsch,J., Bosch,F. and Klug,G. (1994) Cloning of a gene involved in rRNA precursor processing and 23S rRNA cleavage in *Rhodobacter capsulatus*. *J. Bacteriol.*, **176**, 1121–1127.
40. Gregory,S.T., O'Connor,M. and Dahlberg,A.E. (1996) Functional *Escherichia coli* 23S rRNAs containing processed and unprocessed intervening sequences from S*almonella typhimurium*. *Nucleic Acids Res.*, **24**, 4918–4923.
41. Ghora,B.K. and Apirion,D. (1978) Structural analysis and *in vitro* processing to p5 rRNA of a 9S RNA molecule isolated from an *rne* mutant of *E.coli*. *Cell*, **15**, 1055–1066.
42. Li,Z. and Deutscher,M.P. (1995) The tRNA processing enzyme RNase T is essential for maturation of 5S RNA. *Proc. Natl Acad. Sci. USA*, **92**, 6883–6886.
43. Pace,N.R. and Pace,B. (1990) Ribosomal RNA terminal maturase: ribonuclease M5 from *Bacillus subtilis*. *Methods Enzymol.*, **181**, 366–374.
44. Condon,C., Brechemier-Baey,D., Beltchev,B., Grunberg-Manago,M. and Putzer,H. (2001) Identification of the gene encoding the 5S ribosomal RNA maturase in *Bacillus subtilis*: mature 5S rRNA is dispensable for ribosome function. *RNA*, **7**, 242–253.
45. Li,Z., Pandit,S. and Deutscher,M.P. (1998) Polyadenylation of stable RNA precursors *in vivo*. *Proc. Natl Acad. Sci. USA*, **95**, 12158–12162.
46. Coburn,G.A. and Mackie,G.A. (1996) Overexpression, purification, and properties of *Escherichia coli* ribonuclease II. *J. Biol. Chem.*, **271**, 1048–1053.
47. Mott,J.E., Galloway,J.L. and Platt,T. (1985) Maturation of *Escherichia coli* tryptophan operon mRNA: evidence for 3′ exonucleolytic processing after rho-dependent termination. *EMBO J.*, **4**, 1887–1891.
48. McLaren,R.S., Newbury,S.F., Dance,G.S.C. and Causton,H.C. (1991) Messenger RNA degradation by processive 3′–5′ exoribonucleases *in vitro* and the implications for prokaryotic messenger RNA decay *in vivo*. *J. Mol. Biol.*, **221**, 81–96.
49. Newbury,S.F., Smith,N.H. and Higgins,C.F. (1987) Differential mRNA stability controls relative gene expression within a polycistronic operon. *Cell*, **51**, 1131–1143.
50. Spickler,C. and Mackie,G.A. (2000) Action of RNase II and polynucleotide phosphorylase against RNAs containing stem–loops of defined structure. *J. Bacteriol.*, **182**, 2422–2427.
51. Py,P., Higgins,C.F., Krisch,H.M. and Carpousis,A.J. (1996) A DEAD-box RNA helicase in the *Escherichia coli* degradosome. *Nature*, **381**, 169–172.
52. Wang,Y., Duby,G., Purnelle,B. and Boutry,M. (2000) Tobacco VDL gene encodes a plastid DEAD box RNA helicase and is involved in chloroplast differentiation and plant morphogenesis. *Plant Cell*, **12**, 2129–2142.